Available online at www.sciencedirect.com
ScienceDirect
Neural Networks 20 (2007) 690–704
Neural Networks
www.elsevier.com/locate/neunet

A neural model of decision-making by the superior colicullus in an antisaccade task

Vassilis Cutsuridis[a,*], Nikolaos Smyrnis[b,c], Ioannis Evdokimidis[b], Stavros Perantonis[a]

[a] *Computational Intelligence Laboratory, Institute of Informatics and Telecommunications, National Centre for Scientific Research "Demokritos", Agia Paraskevi, Athens GR-15310, Greece*
[b] *Cognition and Action Group, Department of Neurology, National University of Athens, Aeginition Hospital, 72 Vas Sofias Ave., Athens GR-11528, Greece*
[c] *Department of Psychiatry, National University of Athens, Aeginition Hospital, 72 Vas Sofias Ave., Athens GR-11528, Greece*

Received 23 January 2006; accepted 23 January 2007

Abstract

In the antisaccade paradigm subjects are instructed to perform eye movements in the opposite direction from the location of a visually appearing stimulus while they are fixating on a central stimulus. A recent study investigated saccade reaction times (SRTs) and percentages of erroneous prosaccades (towards the peripheral stimulus) of 2006 young men performing visually guided antisaccades. A unimodal distribution of SRTs (ranging from 80 to 600 ms) as well as an overall 25% of erroneous prosaccade responses was reported in that large sample. In this article, we present a neural model of saccade initiation based on competitive integration of planned and reactive saccade decision signals in the intermediate layer of the superior colliculus. In the model the decision processes grow nonlinearly towards a preset criterion level and when they cross it, a movement is initiated. The resultant model reproduced the unimodal distributions of SRTs for correct antisaccades and erroneous prosaccades as well as the variability of SRTs and the percentage of erroneous prosaccade responses.

Keywords: Eye movements; Antisaccades; Buildup neurons; Burst neurons; Nonlinear accumulator model; Decision making; Saccade reaction times; Superior colliculus

1. Introduction

A paradigm often used to investigate decision processes is the antisaccade paradigm (Hallett, 1978), a reaction time task in which the subjects are instructed to perform eye movements in the opposite direction from the location of a stimulus that appears in their right or left peripheral visual field while they are fixating on a central stimulus. Antisaccade reaction times (aSRTs) are longer than would be expected by considering synaptic delays and nerve conduction (Hanes & Schall, 1996) and vary randomly from trial to trial (Everling & Fischer, 1998). The distribution of aSRTs is unimodal and the percentage of erroneous prosaccades towards the peripheral stimulus has been observed to be 25% (Evdokimidis et al., 2002; Smyrnis, Evdokimidis, Stefanis, Constantinidis, & Avramopoulos, 2002).

The slowness and variability of response time (RT) observed in visuomotor tasks has been explained by decision processes involving stochastic accumulation of information (Carpenter & Williams, 1995; Hanes & Schall, 1996; Luce, 1986; McClelland, 1979; Ratcliff, van Zandt, & McKoon, 1999; Reddi & Carpenter, 2000; Usher & McClelland, 2001). In the LATER model (Carpenter & Williams, 1995; Reddi & Carpenter, 2000), a decision signal rises linearly from an initial level in response to incoming information about a stimulus, with its rate varying randomly from trial to trial, until it reaches a fixed criterion or threshold level, at which point a response is initiated (Reddi, Asrress, & Carpenter, 2003). Although the model accurately predicts the latencies of saccades in various simple reaction experimental paradigms (step and countermanding paradigms) as well as the shapes of the distributions (Asrress & Carpenter, 2001; Carpenter & Williams, 1995; Leach & Carpenter, 2001; Reddi et al., 2003;

* Corresponding address: Department of Computing Science and Mathematics, Stirling University, Stirling, Stirlingshire, FK9 4LA, UK. Tel.: +44 1786 467422; fax: +44 1786 464551.
E-mail address: vcu@cs.stir.ac.uk (V. Cutsuridis).

0893-6080/$ - see front matter © 2007 Elsevier Ltd. All rights reserved.
doi:10.1016/j.neunet.2007.01.004

Reddi & Carpenter, 2000), it is unable to predict the error rate in these paradigms. Moreover, the predicting power of the LATER model fails when the model is applied to choice reaction paradigms (e.g. antisaccade task) (see discussion section for details).

The present modelling work addresses some of the limitations of the previous models. It extends an already established leaky competitive neural model of visually guided eye movements in the presence/absence of distractors (Trappenberg, Dorris, Munoz, & Klein, 2001) the inputs of which are modelled as decision signals with linearly rising and randomly varying from trial to trial rates as in the LATER model (Carpenter & Williams, 1995; Reddi & Carpenter, 2000) to explain the variability of response times and the percentage of erroneous responses in the antisaccade task (Smyrnis et al., 2002). The model explains how reactive (erroneous prosaccades) and planned saccades (antisaccades) compete against each other in the intermediate layers of the superior colliculus (SC) and how a decision is formed and executed. The neural circuitry that supports this process simulates successfully responses of buildup neurons (Moschovakis & Karabelas, 1985; Munoz & Wurtz, 1995a, 1995b) and burst neurons of the intermediate layers of the SC (Moschovakis, Karabelas, & Highstein, 1988; Munoz & Wurtz, 1995a, 1995b; Waitzman, Ma, Oprican, & Wurtz, 1991) in the antisaccade task (Everling, Dorris, & Munoz, 1998). Also, the model provides a functional rationale of how buildup cells in these SC layers process decision signals from converging unimodal pathways and how these converging decision signals compete against each other to yield an error and/or a correct eye movement in the form of a phasic response from the burst neurons. Finally, the model suggests why the response times in the antisaccade task are so long and variable and predicts accurately the shapes of correct and error RT distributions as well as their response probabilities.

2. Materials and methods

2.1. General description

An earlier version of the neural model that will be presented in this section was first reported in Cutsuridis, Evdokimidis, Kahramanoglou, Perantonis, and Smyrnis (2003). In the current and more comprehensive model, the preparation of an antisaccadic eye movement consists of two independent and spatially separated decision signals representing the reactive and planned saccade plans. A movement is initiated when these decision signals, represented by the neuronal activity of SC buildup neurons with nonlinear growth rates varying randomly from a normal distribution, gradually build up their activity until reaching a preset criterion level. The crossing of the preset criterion level (Durstewitz, 2003, 2004; Grammont & Riehle, 1999; Matell, Mech, & Nicolelis, 2003; McEchron, Tsend, & Disterhoft, 2003; Roux, Coulmance, & Riehle, 2003; Schultz, Dayan, & Montague, 1997) in turn releases the "brake" from the SC burst neurons and allows them to discharge resulting in the initiation of an eye movement. One of the key assumptions of the model is that in the superior colliculus, the two decision processes are integrated at opposite colliculi locations and they compete with each other via lateral excitation and remote inhibition (Behan & Kime, 1996; Meredith & Ramoa, 1998; Moschovakis et al., 1988; Munoz & Istvan, 1998; Olivier, Dorris, & Munoz, 1999). The growth rate in one decision process slows down when the other decision process is active at the same time.

The neural model proposes that (1) the competition between the SC buildup neurons encoding the decision signals and the randomly varying nonlinear growth rates of the decision processes are the underlying neural mechanisms needed to explain why the aSRTs are so long, (2) the randomly varying nonlinear growth rates of the decision processes generate accurately the correct and error latencies as well as the shape of the distributions seen in the antisaccade task (Evdokimidis et al., 2002; Smyrnis et al., 2002), and (3) the interplay between the criterion level and the randomly varying growth rates of the decision processes can successfully simulate the error rates in the antisaccade task.

2.2. Mathematical formalism

The neural model is a leaky competitive integrator (Amari, 1997; Arai, Keller & Edelman, 1994; Grossberg, 1973; Kopecz, 1995; Kopecz & Schoner, 1995; Taylor, 1999; Trappenberg et al., 2001) of the intermediate layer of the superior colliculus. The neural architecture of the model is described in Fig. 1. Self-excitation and lateral inhibition is assumed between all neurons in both superior colliculi (see Eq. (1)).

Neurons in the model are represented as simple nodes. The central node represents a fixation neuron (black), whereas the peripheral nodes alternatively represent buildup (grey) and burst (white filled) neurons of the right and left superior colliculus. For the sake of simplicity, all three types of neurons lie in the same layer, although experimental (Munoz & Wurtz, 1993, 1995a, 1995b) and computational (Arai et al., 1994; Grossberg, Roberts, Aguilar, & Bullock, 1997) studies have shown that fixation and buildup neurons lie in the same layer of the rostral and caudal pole of the SC respectively, whereas burst neurons lie in a separate layer from the previous two.

Although some of the equations (Eqs. (1)–(3)) presented in this section have been developed before (Trappenberg et al., 2001), new equations are also introduced (Eqs. (4)–(6)). In order to improve the readability of this section, we list in this section all the equations (new and old) of the model.

The internal state $x_i(t)$ of the node with index i is governed by

$$\tau \frac{\mathrm{d}x_i(t)}{\mathrm{d}t} = -x_i(t) + \sum_j w_{ij} A_j(t) + I_p(t) + I_r(t) - u_o + I_n \tag{1}$$

where τ is a time constant, w_{ij} is the synaptic efficacy from node i to node j, A_j is the activity function of node j, I_r and I_p are the reactive and planned inputs that the SC receives from other cortical areas, u_o is a global inhibition term, and I_n is the background noise. The value of u_o is set to zero for the buildup

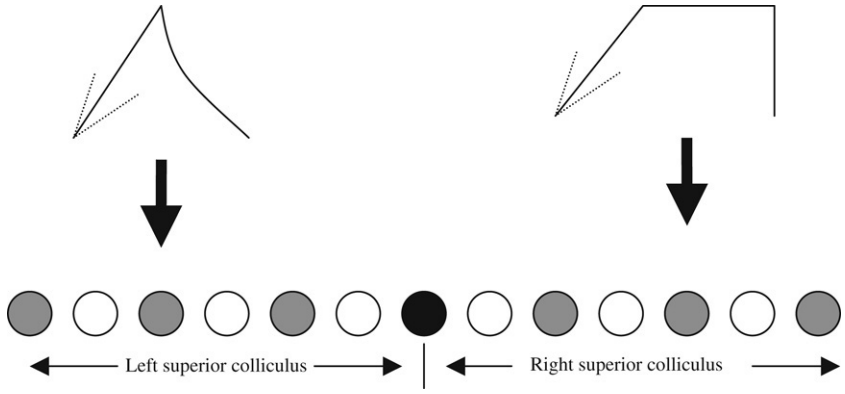

Fig. 1. Model architecture of the intermediate layer of the superior colliculus with fixation cells (black), buildup cells (gray), and burst cells (white). On-centre off-surround connectivity is assumed between all neurons in both superior colliculi (not shown, but see Eq. (1) of Materials and Methods section). Lateral inhibitory interactions between cells mediate the inhibitory effects of inhibitory interneurons (not explicitly modeled in the model) in the superior colliculus. *Vertical solid line* indicates that both right and left superior colliculli consist of a fixation neuron shown in figure as a single fused fixation cell (black). The inputs to this layer are classified as reactive and planned. Their time course is shown schematically corresponding to an onset and offset. Both inputs have a Gaussian spatial distribution (not shown).

nodes, whereas for the burst nodes is set to a large value, since burst neurons are shown to have discharge activity only after the activity of the buildup neurons reaches a certain threshold (Munoz & Wurtz, 1995a). The activity of the burst neurons is restored back to zero only when they surpass an activity level equal to 80% of their theoretical maximum discharge rate (Trappenberg et al., 2001).

The activity function $A_j(t)$ of a node j representing the average membrane potential is given by a sigmoid function

$$A_i(t) = \frac{1}{1 + \exp(-\beta u_i(t) + \theta)} \tag{2}$$

where β is the steepness and θ is the offset of sigmoid (Trappenberg et al., 2001).

The interaction matrix w, which allows for lateral interactions between nodes in the same colliculus and between nodes located in opposite colliculi sites (Meredith & Ramoa, 1998; Moschovakis et al., 1988; Munoz & Istvan, 1998), depends only on the spatial distance between nodes and it is positive for all nodes that excite themselves and negative for nodes that are apart from each other (Trappenberg et al., 2001)

$$w_{ij} = a \exp\left(\frac{-(j-i)^2}{2 \cdot \sigma_a^2}\right) - b \exp\left(\frac{-(j-i)^2}{2 \cdot \sigma_b^2}\right) - c \tag{3}$$

where a, b and c are free parameters and σ_a and σ_b are spatial parameters.

Two competing input signals are integrated in the SC: a planned and a reactive. In the model, the origins of these two input signals differ: the reactive signal is thought to originate from the posterior cortical centres (Munoz & Everling, 2004), and the planned signal from the frontal executive centres of the brain (Munoz & Everling, 2004).

The reactive input signal is governed by a simple differential equation

$$\begin{aligned}
\frac{dI_r}{dt} &= A \cdot |\ \text{slope}_r\ |, \quad \text{if } t \geq t_{\text{on}} + t_r^{\text{delay}} \quad \text{and} \quad I_r \leq I_r^{\max} \\
\frac{dI_r}{dt} &= -\alpha_r A \cdot I_r, \quad \text{if } t \geq t_{\text{on}} + t_r^{\text{delay}} \quad \text{and} \quad I_r > I_r^{\max} \\
\frac{dI_r}{dt} &= -\alpha_r A \cdot I_r, \quad \text{if } t < t_{\text{on}} + t_r^{\text{delay}}
\end{aligned} \tag{4}$$

where α_r are the integration strengths, $I_{r,\max}$ is a theoretical maximum allowed activity for the reactive input, A is the strength of the rising phase and slope_r is the slope of the linear rising phase of the reactive input. The reactive input reflects the sensory information reaching the SC without extensive information processing and it is taken to follow closely the onset of a visual stimulus in the periphery with a delay $t_{r,\text{delay}}$.

The planned input signal has also a linear rising phase before it reaches its theoretical maximum value and it is governed by

$$\begin{aligned}
I_p &= A \cdot |\text{slope}_p \cdot t|, \quad \text{if } t_{\text{on}} + t_p^{\text{delay}} \leq t \leq t_{\text{off}} + t_p^{\text{delay}} \\
&\quad \text{and} \quad I_p < I_p^{\max} \\
I_p &= A \cdot I_p^{\max}, \quad \text{if } t_{\text{on}} + t_p^{\text{delay}} \leq t \leq t_{\text{off}} + t_p^{\text{delay}} \\
&\quad \text{and} \quad I_p \geq I_p^{\max} \\
I_p &= 0, \quad \text{else}
\end{aligned} \tag{5}$$

where $I_{p,\max}$ is the theoretical maximum activity of the planned input, A is the strength of the planned input and $|\text{slope}_p|$ is the absolute value of the slope of the planned input rising phase. The planned input reflects the processing of the planned antisaccade by higher processing centres such as the frontal eye fields (FEF), the supplementary eye fields (SEF), and the dorsolateral prefrontal cortex (DLPFC) to determine the behaviour response that would be appropriate for the given task instruction and it is considered to take longer ($t_p^{\text{delay}} > t_r^{\text{delay}}$) for processing than the reactive input due to additional cortical processing.

The strength of both planned and reactive signals is given by

$$A = \exp\left(\frac{-(i-j)^2}{2\sigma_A^2}\right) \quad (6)$$

where i and j are the indices of nodes and σ_A is the standard deviation of the Gaussian. The width of the Gaussian was derived from the shape of movement fields of saccade-related neurons in the monkey SC (Munoz & Wurtz, 1995b; Trappenberg et al., 2001).

In the model, the initial phases of both the reactive and the planned inputs were modelled with an initial linearly rising phase (Hanes & Schall, 1996; Reddi & Carpenter, 2000) until they both reached their corresponding theoretical maximum value. The slope of each input varied randomly from a normal distribution with mean (μ) and standard deviation (σ) and with a different rate for each run (trial) (the process by which the mean and standard deviation were determined is explained in the Results section) and it was generated using MATLAB's *normrnd* routine. The remaining phases of the temporal profiles of the two inputs followed the Kopecz (1995) observations.

The afferent delays, t_{delay}, of the reactive and planned inputs were chosen so that the simulations resemble the cell data of macaque monkeys (Dorris, Pare, & Munoz, 1997). The latency of the reactive response was set at 70 ms (Dorris et al., 1997), whereas the latency for the higher cortical response was set at 120 ms (Trappenberg et al., 2001). The 50 ms difference in these latencies was reported by Becker (1989) and it has been explained as an additional cortical processing of the planned signal before it reaches the superior colliculus. Saccade reaction times (SRTs) were estimated to be the time interval from the onset of peripheral stimulus till the time the activity of the burst neurons deviated from zero plus 20 ms (approximate time required for burst neuron signal to reach the eye muscles) (Sparks, 1978).

Finally, to simulate the random fluctuations in the waveforms derived from the cell recordings, a normally distributed random variable, $I_n = \alpha_n N(0, 1)$ with strength α_n is introduced in Eq. (1).

2.3. Implementation

The simulations were performed on a Pentium IV 3 GHz PC with MATLAB's version R13 installed. The whole system of differential and algebraic equations was implemented in MATLAB (The MathWorks, Inc, Natick, MA). Differential equations were integrated numerically using MATLAB's ordinary differential equation solver, ode45 (an implicit solver based on the Dormand–Prince pair method (Dormand & Prince, 1980). The relative (error) tolerance was set to 10^{-4}.

2.4. Experimental data

The psychophysical data used in this study were collected in another study (Evdokimidis et al., 2002; Smyrnis et al., 2002). Details of the experimental procedure used for the collection of these data are described therein (Evdokimidis et al., 2002; Smyrnis et al., 2002). Briefly, 2006 conscripts of the Greek Air Force (age 18–25) performed 90 trials of the antisaccade task. Each trial started with the appearance of a central fixation stimulus. After a variable period of 1–2 s, the central stimulus was extinguished and a peripheral stimulus appeared randomly at one of nine distances (2°–10° at 1° intervals) either to left or to the right of the central fixation stimulus. The subjects were instructed to make an eye movement to the opposite direction from that of the peripheral stimulus as quickly as possible. No accuracy constraints were applied. The correct or error saccade reaction time (SRT) was measured in each trial for every subject. Saccade reaction time was defined as the time taken from the first appearance of the peripheral stimulus 'till the first detectable eye movement. Trials with reaction times <80 ms were excluded as anticipations and trials with reaction times >600 ms were excluded as no response trials.

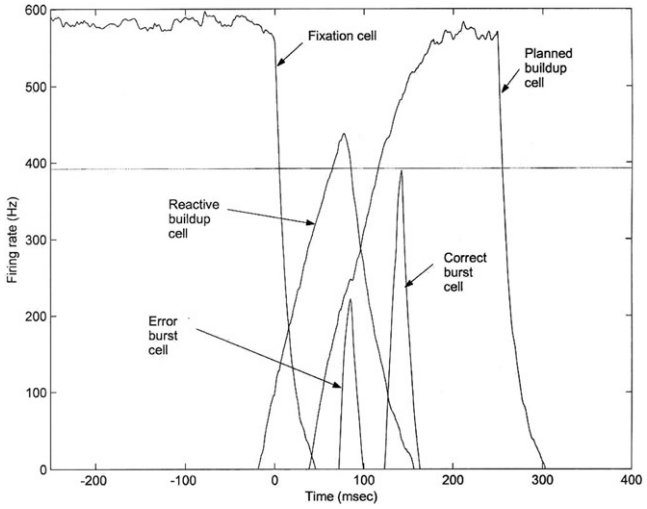

Fig. 2. *Top*. Composite simulated discharge activities of fixation, buildup (encoding reactive and planned saccade plans) and burst (generating erroneous and correct antisaccades) cells in the visually-guided (step) antisaccade task. Horizontal solid line depicts the threshold level. Time units are in ms.

In this behavioural setting (Evdokimidis et al., 2002; Smyrnis et al., 2002) only three eye movement behaviours were observed: (1) the subject makes an antisaccade, (2) the subject makes an error prosaccade only (very rare), (3) the subject makes an error prosaccade followed by a correct antisaccade. However, at no time during the antisaccade task was it ever observed for a subject to make a correct antisaccade followed by an error prosaccade in the same trial.

2.5. Clustering analysis

Ratcliff (1979) presented a method for obtaining group reaction time distributions from experiments in which there were as few as 10 observations per subject cell. His method essentially involved estimating latency quartiles for each subject and then averaging these over the group of subjects. Ratcliff (1979) showed that the parameters derived from the group distributions were the same as the parameters used to generate the individual pseudo-subject distributions and that group distributions provide an excellent summary of

Table 1
Range of model parameters

Parameters	Description	Values
N	Number of nodes in the model	101
β	Steepness of activation function	0.07
θ	Offset of activation function	0
τ	Time constant	15
a	Free parameter	144
b	Free parameter	48
c	Free parameter	16
σ_a	Free parameter	0.6 mm
σ_b	Free parameter	1.8 mm
a_n	Strength of noise input	20
$I_{p,\max}$	Maximum value for planned input	600 spikes/s
$I_{r,\max}$	Maximum value for reactive input	500 spikes/s
$t_{p,\text{delay}}$	Delay time for planned input reflecting extra time required for cortical processing	120 ms
$t_{r,\text{delay}}$	Delay time for reactive input reflecting extra time required for cortical processing	70 ms
t_{on}	Time value, where inputs are turned on	120 ms (endo) 70 ms (exo)
t_{off}	Time value, where inputs are turned off	600 ms
σ_A	Standard deviation of Gaussian distribution function used for the rising phases of reactive and planned inputs	1.5
a_r	Decay term of reactive input	
μ_1	Mean of normal distribution from which the slope of planned input takes values	Variable (see Table 2)
σ_1	Standard deviation of normal distribution from which the slope of planned input takes values	Variable (see Table 2)
μ_2	Mean of normal distribution from which the slope of reactive input takes values	Variable (see Table 2)
σ_2	Standard deviation of normal distribution from which the slope of reactive input takes values	Variable (see Table 2)
u_o	Global inhibition	0 (buildup nodes) 100 (burst nodes)

distributional information for the group and don't introduce any systematic bias into the estimate of shape.

In our study, the median RT and the inter-quartile range for antisaccades and error prosaccades of all 2006 conscripts were grouped into ten groups after performing clustering analysis using the STATISTICA software version 5.5 (StatSoft, Inc, Tulsa, OK). The purpose of the cluster analysis was to partition the observations into groups ("clusters") so that the pairwise dissimilarities between those assigned to the same cluster tend to be smaller than those in a different cluster. We arbitrary chose ten clusters because we wanted each cluster to have a sufficiently large number of individuals (ranging from 30 individuals to 240 individuals in each cluster).

3. Results

The first part of this section examines the activities of fixation, burst and buildup neurons in the antisaccade task. The second part examines the shapes of the antisaccade and error prosaccade SRT distributions and the antisaccade response probabilities for all individuals on the average. The third part discusses the shapes of the antisaccade and error prosaccade SRTs and the antisaccade response probabilities for ten groups of individuals and how they compare with the experimental ones.

3.1. Burst and buildup cell simulations

The simulations of the time course of fixation, burst and buildup cell activities in the antisaccade task are summarized in Fig. 2. The values of the parameters used in this simulation are depicted in Table 1. All simulation results reported in this paper were produced with $N = 101$ nodes, 50 buildup, 50 burst, and one fixation. The spatial arrangement of the nodes can be seen in Fig. 1.

Fig. 2 shows composite simulated discharge activities of fixation, buildup and burst neurons from a simulation run of the antisaccade task. In this particular run, the threshold level (horizontal line at about 400 Hz) was carefully adjusted, so that both buildup nodes encoding the reactive and planned inputs crossed the threshold and an erroneous prosaccade (*error burst*) was initiated followed by a correct saccade (*correct burst*). In the beginning of each simulation run, the planned input, reflecting the decision of each subject to fixate on the central stimulus, is presented to the fixation node. During the fixation period, only the fixation node is allowed to have tonic activity that lasts for the entire fixation period (Munoz & Wurtz, 1993). In contrast with the gap antisaccade task, in this antisaccade task the fixation tonic activity prevents the buildup nodes from having any preparatory activity (Dorris et al., 1997; Everling et al., 1998). In the antisaccade experimental task described earlier, when the peripheral stimulus appears either on the left or right side of the subject's visual field, then the subject has to make an eye movement to the opposite direction of the visually presented stimulus. In the model, the appearance of the peripheral stimulus causes the fixation node's activity to start decaying, while the buildup nodes' activities start to rise. The activity of the fixation node reaches zero slightly before the burst neuron activity starts to grow. Once the activities of the buildup nodes reach a preset threshold value (80% of their theoretical maximum activity (see Table 2) (Durstewitz, 2003, 2004; Grammont & Riehle, 1999; Matell et al., 2003;

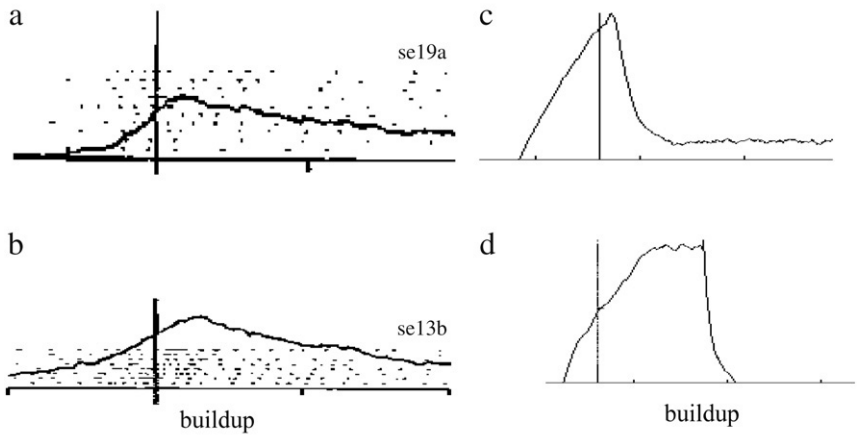

Fig. 3. (a) Burst cell response (reproduced with permission from Everling et al. (1999)) and (b) buildup cell response (reproduced with permission from Everling et al. (1999)) compared with qualitative simulations of a (c) burst and (d) buildup cell responses in a visually guided antisaccade paradigm. a–d, All plots are aligned to the onset of the saccade. The graphs show cell activity as it changes over time. Note that a saccade is initiated before both buildup and burst cell activities reach their peak values.

McEchron et al., 2003; Roux et al., 2003; Schultz et al., 1997; Trappenberg et al., 2001), the inhibition is removed from the burst neurons allowing them to discharge with high frequency (Munoz & Wurtz, 1995a, 1995b). The onset of the burst activity reflects the onset of the saccade movement, exactly as it observed in experimental studies (Munoz & Wurtz, 1995a, 1995b). Once the activity of the burst neurons reaches 80% of their theoretical peak value (see Table 1), instant reestablishment of inhibition is applied to the burst neurons and their activity returns to zero (Trappenberg et al., 2001). When the burst activities reach zero, the activities of the buildup neurons start decaying (Munoz & Wurtz, 1995a, 1995b) and the saccade-related pause of fixation cell discharge is lift off and the fixation node activity starts to grow again (Munoz & Wurtz, 1993).

In each simulation run, the reactive and planned inputs are delivered to buildup nodes located on opposite collicular sites. So, when the peripheral stimulus appears on the right side of the visual field and the subject needs to make an eye movement to the left side, then the primary buildup node contralateral to the peripheral stimulus encodes the reactive input (*error decision*), whereas the primary buildup node ipsilateral to the peripheral stimulus encodes the planned input (*correct decision*), and vice versa. To simulate such behaviour in our model, a random node to right of the central stimulus and a random node to the left of the central stimulus are chosen in each trial. Then, randomly the right or the left hemifield is chosen and subsequently the previously randomly selected node in the contralateral hemifield is marked as the peripheral stimulus site. That node and its nearest neighbours are then chosen to integrate the reactive input, whereas the previously ipsilateral randomly selected node and its nearest neighbours are chosen to integrate the voluntary input. The reactive input is delivered to buildup nodes with a time delay of 70 ms after stimulus presentation, whereas the planned input is delivered to buildup nodes with a time delay of 120 ms after stimulus presentation. The 50 ms delay between the two inputs matched the experimental observations of Becker (1992). The strengths of both inputs have a Gaussian spatial shape, so that when the input is centred at node i, its neighbouring nodes received a percentage of that input that decreased as the spatial distance from the central node increased. For example, if the buildup node number 13 on the ipsilateral to the peripheral stimulus SC received the planned input, then its neighbouring buildup nodes 11 and 15 received a proportion α smaller than the maximum strength of the planned input and nodes 9 and 17 received a proportion β ($\beta < \alpha, \beta \ll \max$) of the maximum strength of the planned input. Similarly, for the buildup nodes that received the reactive input. The width of the Gaussian is derived from the shape of movement fields of saccade-related neurons in the monkey SC (Munoz & Wurtz, 1995b). The buildup nodes on remotely opposite colliculi sites are then allowed to compete with each other until their activities reached and crossed a fixed threshold level, which caused the 'brake' from the burst nodes to be removed and an eye movement to be initiated.

Fig. 3 shows experimentally recorded burst and buildup cell responses (Everling et al., 1998) compared with qualitative simulations of burst and buildup cell responses in a visually guided antisaccade paradigm. The activities of both simulated and experimental activities are aligned to the onset of an antisaccade eye movement. Briefly, Everling et al. (1998) trained monkeys on a pro/anti-saccade paradigm in which they either had to generate a saccade toward the visual stimulus or an antisaccade away from the visual stimulus to its mirror position depending on the colour of the initial fixation point, while they recorded from the monkeys' superior colliculus (SC), in order to determine whether the SC is involved in the generation of antisaccades. Everling and colleagues study (1998) showed that the antisaccade task involves the attenuation of preparatory and stimulus-related activity in the SC to avoid unwanted prosaccades. The model is able to qualitatively simulate the activities of the burst and buildup neurons (Fig. 3c, d).

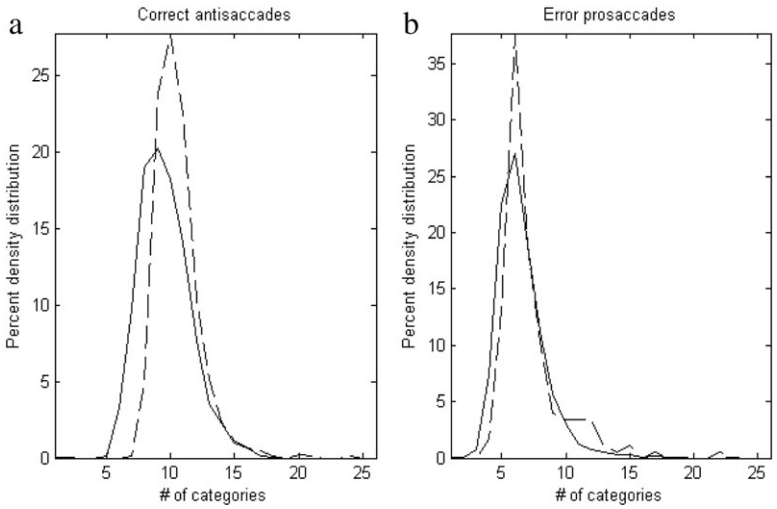

Fig. 4. Plots of correct percent density distribution (y-axis) vs number of categories (x-axis) for all 2006 subjects. Dashed lines: simulated correct percent density distribution plot. *Solid lines*: experimental correct percentage density distribution plot.

3.2. Comparison with behavioural data using the average data for all subjects

We estimated the median reaction times, the shapes of the RT distributions of the correct antisaccades and error prosaccades as well as the response probabilities for all 2006 individuals on the average by allowing the model to run for 1200 trials. In each trial, the slope of the reactive input took values from a normal distribution with mean (μ_1) and standard deviation (σ_1), whereas the slope of the planned input took values from another normal distribution with mean (μ_2) and standard deviation (σ_2). The mean values of the two normal distributions were chosen by a trial-and-error process. Initially, the model was allowed to run for single trials, where the slopes of both the reactive and planned inputs were carefully adjusted, so that the model could give correct antisaccade and error prosaccade reaction times that closely resembled the experimental ones (for experimental values see inside parentheses of last row in Table 2. These slope values were then used as mean values for the two normal distributions. Standard deviation values σ_1 and σ_2 were approximated so that most of the produced correct antisaccade and error prosaccade reaction times were greater than 80 ms and less than 600 ms. Then, MATLAB's *normrnd* routine was used to generate random slope values for each of two distributions equal to the total number of trials (1200 in this case).

The threshold was set to 80% of the maximum activity of the buildup neurons (Durstewitz, 2003, 2004; Grammont & Riehle, 1999; Matell et al., 2003; McEchron et al., 2003; Roux et al., 2003; Schultz et al., 1997; Trappenberg et al., 2001); see Table 1. Trials with response times less than 80 ms and greater than 600 ms were excluded. Saccade reaction time (SRT) was estimated as the time taken from the first appearance of the peripheral stimulus 'till the time burst node activity started to deviate from zero. An additional 20 ms efferent delay was also added, which it was a typical value found in recording and stimulation studies (Munoz & Wurtz, 1995a; Sparks, 1978). All three experimentally observed eye movement behaviours (see *Experimental data*) were produced by our model. The model at no time was able to produce a correct antisaccade followed by an error prosaccade, exactly as it is observed in antisaccade tasks (Evdokimidis et al., 2002; Smyrnis et al., 2002). The model clearly demonstrated that there is no need of a top-down inhibitory signal which will prevent the expression of the correct antisaccade when the error prosaccade is expressed first. The median antisaccade and error prosaccade response times and the error rate for the simulated data and the corresponding values derived from all 2006 individuals are displayed in Table 2 (last row). It can be seen that the average response times and error rate simulated values approximate the experimental ones.

We compared the SRT distributions of the real experimental data with the simulated SRT distributions for all 2006 subjects by normalizing the experimental and simulated correct and error SRT distributions. More specifically, the time interval between the 80 and 600 ms was divided into twenty-six categories, each lasting 20 ms (e.g. category 1 was between 80 and 100 ms, category 2 between 100 and 120 ms, and so forth). For each category we calculated its percent relative frequency of response times. Plots of the simulated and experimental correct antisaccade and error prosaccade % density distributions of response times for all 2006 subjects are depicted in Fig. 4. The mean frequency was then calculated. The discrepancy in each category between the simulated and experimental correct and error distributions was measured by the squared difference between the observed (simulated) and the expected (experimental) frequencies divided by the expected frequency ((Observed − Expected)^2/Expected). The χ^2 value was the sum of these quantities for all categories. The rejection region was set at $\chi^2 \geq \chi^2_{0.05}$. The χ^2 test of homogeneity tested the null hypothesis of whether the simulated and experimental normalized distributions of SRTs for antisaccades and error prosaccades differ between them. No significant difference was shown (see last row of Table 3).

Table 2
Mean and standard deviation of slopes of planned and reactive inputs and simulated correct median, error median, and error rate for average and all ten groups

	μ_1	σ_1	μ_2	σ_2	Threshold	Median RT of antisaccades	Median RT of error prosaccades	Percent antisaccade error rate
Group1	4.0	1.0	3.6	0.9	416	294.174 (288.16)	279.541(265.20)	13.04 (16.15)
Group 2	3.6	1.0	5.3	1.5	392	276.50 (279.21)	202.97 (201.96)	38.62 (39.07)
Group 3	3.5	0.9	5.5	1.6	400	281.89 (280.91)	212.54 (201.92)	20.15 (23.73)
Group 4	4.9	1.3	5.8	1.5	400	251.30 (249.27)	209.90 (211.65)	12.41 (12.02)
Group 5	4.7	1.8	5.0	1.3	408	254.80 (242.40)	212.99 (216.66)	24.27 (17.02)
Group 6	3.4	0.8	6.8	1.8	384	282.38 (288.44)	188.10 (193.66)	23.93 (28.86)
Group 7	3.9	0.9	7.5	2.0	376	263.10 (251.79)	180.63 (175.53)	20.87 (24.79)
Group 8	2.1	0.5	4.6	1.3	406	365.69 (349.42)	218.99 (221.36)	37.00 (34.58)
Group 9	7.3	2.3	7.5	2.1	367	218.20 (213.58)	177.85 (172.77)	27.36 (24.92)
Group 10	2.8	0.9	2.4	0.6	432	327.56 (307.5)	331.07 (326.99)	20.05 (21.81)
All subjects	3.7	0.8	5.9	1.6	493	274.75 (275.07)	198.61 (200.67)	21.53 (24.3)

Units: correct SRT (ms), error SRT (ms). Values in parentheses stand for experimental values.

Table 3
Values of χ^2 test of homogeneity between correct and error experimental and simulated percentage density distributions for antisaccades and error prosaccades

	Antisaccades	Error prosaccades
Group 1	36.15	34.92
Group 2	90.5*	33.56
Group 3	32.16	32.89
Group 4	56.06*	96.24*
Group 5	35.21	24.18
Group 6	31.82	27.97
Group 7	30.34	21.82
Group 8	36.46	35.67
Group 9	36.99	23.15
Group 10	33.88	83.57*
All subjects	37.52	34.19

χ^2 values marked with an asterisk indicate a significant difference between the simulated and the observed RT distributions. *Rejection region*: $\chi^2 \geq \chi^2_{0.05}(37.65)$. The degrees of freedom were 25.

3.3. Comparison with behavioral data for the 10 groups of subjects

Once again the reactive and the planned inputs were modelled with an initial linearly rising phase. The slope of each linearly rising phase of each input was varied randomly from a normal distribution with mean (μ) and standard deviation (σ) and with a different rate for each run (trial) as it was described in the previous section. MATLAB's *normrnd* routine was used once more to generate random slope values for each of two distributions equal to the total number of trials for which the model was chosen to run (see below). The threshold was adjusted, so that the simulated error rate closely matched the observed. Its value was set to a different value for each group, but it was kept fixed across trials for each group.

The model was allowed to run for 1000 trials. Trials with response times less than 80 ms and greater than 600 ms were excluded. All three experimentally observed eye movement behaviours (see *Experimental data*) were produced by our model. All three behaviours were produced without the need of a top down inhibitory signal as it often experimentally postulated and theoretically hypothesized to exist (Munoz & Everling, 2004). The median antisaccade and error prosaccade RTs and the error rate for the simulated data for each group and the corresponding values for the experimental groups are displayed in Table 2. It can be seen that the simulated values approximate the experimental ones in most cases.

In order for each group to compare the SRT distributions of the real experimental data with the simulated SRT distributions, we used the procedure described in the previous section. More specifically, we normalized the SRT distribution of each subject data and then added the normalized distributions for all subjects belonging to the same group. For each category we calculated its percentage relative frequency of response times. Plots of the simulated and experimental correct antisaccade and error prosaccade % density distributions of response times for all ten groups are displayed in Figs. 5 and 6. The mean frequency for all subjects in a group was then calculated. The discrepancy in each category between the simulated and experimental correct and error distributions was measured by the squared difference between the observed (simulated) and the expected (experimental) frequencies divided by the expected frequency ((Observed−Expected)^2/Expected). The χ^2 value was the sum of these quantities for all categories. Once again, the rejection region was set at $\chi^2 \geq \chi^2_{0.05}$. The χ^2 test of homogeneity showed a significant difference in two of the ten comparisons for antisaccade RT distributions and two of the ten comparisons for the error prosaccade RT distributions (see Table 3).

4. Discussion

4.1. General issues

One of the most universal ways to represent a decision signal is with growth processes that gradually build up their activity until reaching a fixed threshold activation level (Mazurek, Roitman, Ditterich, & Shadlen, 2003; Mazurek & Shadlen, 2002). A growth process may have many different psychological and physiological interpretations. For example, it is assumed that there is a steady flow of information about which of the many movement instructions is presented, providing support for a fixed accumulating rate (Carpenter & Williams, 1995). A substantial body of experimental evidence indicates that neurons in area MT represent the critical sensory signals that monkeys use to base their judgement of random

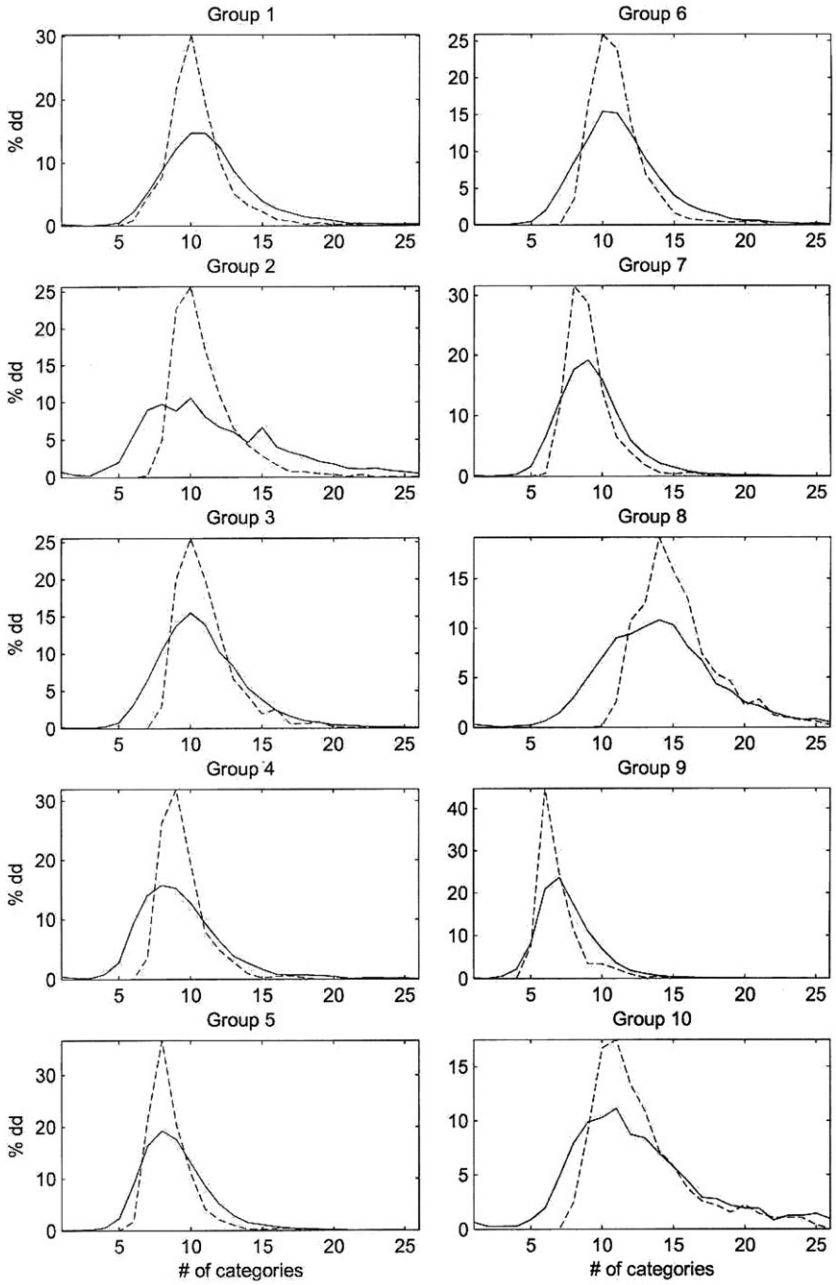

Fig. 5. Plots of correct percentage density distribution (y-axis) vs number of categories (x-axis) for all ten groups. *Dashed lines*: simulated correct percentage density distribution plots for all ten groups. *Solid lines*: experimental correct percentage density distribution plots for all ten groups.

dot motion (Britten, 2003; Parker & Newsome, 1998). Other neurophysiological data show that many neurons in the frontal eye field (FEF) area related to saccadic eye movements can be considered as accumulators building their activity before movement starts. The primary function of these accumulators is to make preparations for saccadic eye movements (Hanes & Schall, 1996). Also, one third of the saccade-related cells in the monkey SC begin to build up their activity after the signal to make a saccadic eye movement is presented and continue to discharge until the beginning of the movement (Munoz & Wurtz, 1995a, 1995b). As the number of possible targets decreases, the level of neuronal activity preceding the saccadic eye movement also increases (Basso & Wurtz, 1998). These buildup cells, which seem to be involved in the preparation, rather than in execution of eye movement, are good candidates for accumulators that implement the decision process about the required movement parameters.

Our model which instantiates this idea of the decision in the antisaccade task is based on the time integral of sensory-motor evidence represented by neurons in the superior colliculus (SC) area. The simulations described in this paper do not simply test the idea, but also explore its implications. The model provides insights into the neural mechanisms that underlie integration of information and exposes important features of

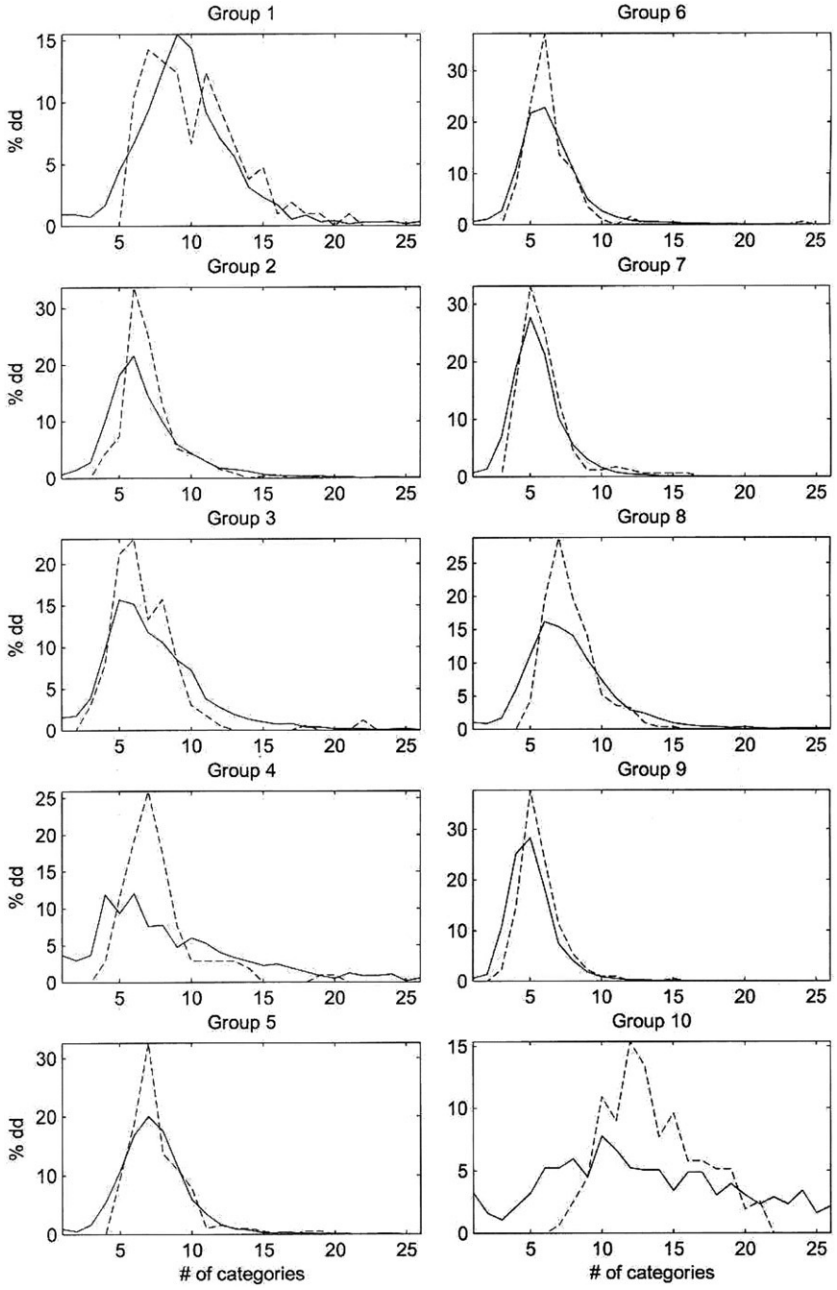

Fig. 6. Plots of error percent density distribution (y-axis) vs number of categories (x-axis) for all ten groups. Dashed lines: simulated error percentage density distribution plots for all ten groups. Solid lines: experimental error percentage density distribution plots for all ten groups.

the data, furnishes novel interpretations, and makes predictions that may motivate future experiments. In what follows, we explain the rationale behind the assumptions taken in the model, and explore the model's predictions, limitations and future extensions.

4.2. Model assumptions and predictions

The model presented herein offers an alternative view for saccadic eye movement generation that is supported by experimental evidence. The model isn't concerned with visuomotor transformations in the SC (Grossberg et al., 1997). It is primarily concerned with what happens after the motor commands are formed, how the two processes of reactive saccadic suppression and voluntary response generation are represented in the brain and how they are handicapped in the antisaccade task.

In our model, we assumed that the rising phases of the planned and reactive inputs were linear and that they took values from two normal distributions with different means and standard deviations. Such an assumption is consistent with known neurophysiology of saccadic eye movements. In the frontal eye fields of monkeys there are populations of visuomotor neurons that begin to fire in advance of saccades,

with their activity rising linearly upon presentation of a suitable target stimulus (Hanes & Schall, 1996; Kim & Shadlen, 1999; Schall & Hanes, 1998). Buildup neurons in the monkey SC begin to linearly build up their activity after the signal to make a saccade is presented (Everling et al., 1998; Munoz & Wurtz, 1995b). In all these studies, the rate of rise varies randomly from trial to trial and the saccade is initiated when this activity reaches a fixed threshold (Hanes & Schall, 1996; Reddi & Carpenter, 2000).

In the model, a fixed 50 ms latency difference in the onsets of the buildup neurons encoding the two inputs was further assumed and supported by experimental evidence (Becker, 1989, 1992). Furthermore, the assumed origins of the two inputs allowed for such a latency difference. The reactive signal was thought to originate from the projection of the posterior parietal cortical centers to the SC, whereas the planned signal was thought to be the inverted saccade vector from the projection of the posterior parietal cortical centres to the frontal executive centres of the brain, which in turn projected to the SC (Munoz & Everling, 2004).

Once the reactive and planned inputs were integrated in the SC model, the activities of the buildup neurons encoding the reactive and planned inputs were allowed, while competing each other, to grow nonlinearly, until they reached a predefined threshold level (80% of their theoretical maximum activities) (Hanes & Schall, 1996; Reddi & Carpenter, 2000). At that moment, the burst neurons began to fire at high frequencies, whose responses were presumed to last for the duration of the eye movement (Sparks, 2002). Similar behaviour has been observed in experimental working memory, operant or trace conditioning tasks, where the climbing activities of neurons when exceeding some rather constant firing rate threshold caused an abrupt increase or decrease in the firing rate of cortical and subcortical postsynaptic neurons around the expected time of occurrence of an event (Durstewitz, 2003; Grammont & Riehle, 1999; Matell et al., 2003; McEchron et al., 2003; Roux et al., 2003; Schultz et al., 1997).

The activity of the buildup neurons encoding the planned input (antisaccade) was considered in all trials to be greater than the fixed threshold and greater than the activity of the buildup neurons encoding the reactive input (error prosaccade). Behaviorally this meant that the antisaccade was always expressed even when the error saccade was first expressed. Although there is no neurophysiological evidence supporting such an assumption, we consider it to be reasonable because it reflected the instruction that each subject received in the beginning of each task that they had to make a voluntary eye movement to the opposite direction of the presented stimulus. Such an assumption is further supported by behavioral evidence (Evdokimidis et al., 2002; Smyrnis et al., 2002), which showed that subjects were always able to correct an error prosaccade in the antisaccade task.

Finally, a fixed threshold across all trials (Hanes & Schall, 1996) in each virtual subject, but variable across all virtual subjects reflecting inter-subject variability was assumed. Experimental evidence supporting the fixed threshold level assumption comes from recordings from the frontal eye fields and the superior colliculus areas of monkeys (Everling, Dorris, Klein, & Munoz, 1999; Everling et al., 1998; Hanes & Schall, 1996). Hanes and Schall (1996) observed that movements were initiated *if and only if* the neural activity reached a specific and *constant threshold activation level*. Stochastic variability in the rate at which neural activity grew toward that threshold resulted in the distribution of reaction times. In Everling et al. (1999), the role of the primate superior colliculus in preparation and execution of gap and overlap antisaccades and prosaccades was investigated. The discharges of visual, buildup, burst and fixation neurons in both conditions were measured and it was observed that the responses of the buildup neurons in the prosaccade task are greater than the responses of the buildup neurons in the antisaccade task. Everling et al. (1999) tried to explain this finding by suggesting the presence of two separate threshold levels for each set of buildup neurons. We believe that their finding could have been better explained, if they have assumed in the antisaccade task that the reactive and volitional signals are integrated into two different populations of buildup neurons that are contralateral to each other, whereas in the case of the prosaccade, the reactive and volitional signals are integrated in the same set of neurons. This might have been a reason of why the responses of neurons in the prosaccade task are greater than the responses of neurons in the antisaccade task. In another study, Everling et al. (1999) reported that the responses of neurons encoding the erroneous prosaccade are greater in magnitude than the responses of neurons encoding the correct antisaccade in the gap antisaccade task, indicating the presence of two separate threshold levels. We believe that one reason for such a difference could be the fact that anticipatory neuronal activity is present before the target appearance in all gap saccade tasks. In the antisaccade with no gap between offset of the central fixation and the target appearance no such anticipatory activity is present. If one compares the neuronal activity for erroneous and correct antisaccade neurons after the target appearance in this no gap condition (Fig. 3 in Everling et al., 1999) it can be seen that the two activities are approximately equal.

Using the above experimentally verified assumptions in a competitive model of the SC we offered a functional rationale at the SC neuronal population level of why the antisaccadic reaction times are so long and variable and simulated accurately the correct antisaccade and error prosaccade latencies, the shape of RT distributions with their characteristic skewness towards the higher response times and the error probabilities (see Figs. 4–6 and Tables 2 and 3). A χ^2 test of homogeneity of experimental and simulated SRT distributions showed that only four out of 22 (11 correct antisaccade groups and 11 error prosaccade groups) groups show significant difference. A closer look at those distributions shows that the left tail of the theoretical distribution curves are not matching exactly the left tail of the experimentally derived curves. This means in terms of temporal values that the model can produce SRTs as low as a maximum lower bound (approximately 120 ms). Hence, our model models very well the visually guided regular antisaccade responses, but not the *visually guided express antisaccade* responses. This finding is supported

by experimental evidence (Fischer & Weber, 1992; Pare & Munoz, 1996) showing that express saccades are produced from different neurophysiological mechanisms than the regular antisaccades.

The major prediction of our model is that there is no need of a top-down inhibitory signal that prevents the error prosaccade from being expressed, thus allowing the antisaccade to be released. Our work suggests that the preparation of an antisaccadic eye movement is the result of two competing decision signals representing the reactive and planned saccades arising from different cortical areas (Godijin & Theeuwes, 2002; Hunt, Bettina, von Muhlenen, & Kingstone, 2004; Trappenberg et al., 2001), which are integrated at opposite colliculi sites. An eye movement is initiated when these decision signals which are represented by the activity of SC buildup neurons with nonlinear growth rates varying from trial to trial randomly from a normal distribution, gradually buildup their activity until they reach a preset threshold level (Carpenter, 2000; Hanes & Schall, 1996). The crossing of the threshold level by the buildup neurons removes the "brake" from the SC burst neurons and allows them to discharge and hence an eye movement to be initiated (Munoz & Wurtz, 1995a, 1995b). This finding challenges the currently accepted view of saccade generation in the antisaccade task, which requires a top-down inhibitory signal to suppress the erroneous prosaccade after the antisaccade has been expressed (Munoz & Everling, 2004). In the neurophysiological studies of the antisaccade task in primates (Funahashi, Chafee, & Goldman-Rakic, 1993; Hikosaka, Takikawa, & Kawagoe, 2000; Hikosaka & Wurtz, 1983; Munoz & Everling, 2004; Munoz & Fecteau, 2002; Shook, Schlag-Rey, & Schlag, 1990) such a top-down inhibitory signal was never documented (for a review see Munoz and Everling (2004)).

4.3. Comparison with other models

Our model introduces new ideas while incorporating and extending ideas from previous models. The idea of a decision process involving accumulation of information as a way of modeling the variability in RT observed in behavioural paradigms has been discussed before (Carpenter & Williams, 1995; Hanes & Schall, 1996; Luce, 1986; McClelland, 1979; Ratcliff et al., 1999; Reddi & Carpenter, 2000; Usher & McClelland, 2001). The Race/LATER model of Carpenter and colleagues is the most successful representative of these types of models. As it was previously mentioned, although the Race/LATER model of Carpenter and colleagues (Carpenter & Williams, 1995; Reddi & Carpenter, 2000) is very successful at predicting SRTs and the shapes of their distributions in *simple reaction tasks* (Asrress & Carpenter, 2001; Carpenter & Williams, 1995; Leach & Carpenter, 2001; Reddi et al., 2003; Reddi & Carpenter, 2000), its predicting power breaks down when it is applied in choice reaction time tasks (e.g. antisaccade task).

Let's now try to apply the LATER model to the constraints of the antisaccade task presented in our study and detailed in Section 4.2. As was mentioned earlier, in the antisaccade task, only three behaviours are observed: (1) the subject makes the correct antisaccade, (2) the subject makes the error prosaccade and (3) the subject makes first the error prosaccade and then corrects with the antisaccade. Since there is no competition between the two decision signals (*erroneous prosaccade* and *correct antisaccade*) in the LATER model, then the signal that first exceeds the threshold is the winner. This signal will also be the cue for interrupting the model run and ending the trial. We identify the following three scenarios: (1) the slope of the error decision is larger than the slope of correct decision, (2) the slope value of the correct decision is larger than the slope of the error decision, and (3) the slope values of the two decision signals are equal. In scenario 1, the error decision will reach first the threshold and hence the subject will make the error prosaccade. The trial will end without the correct decision crossing the threshold. In scenario 2, the correct decision will cross the threshold first and hence the subject will make the correct antisaccade. The trial will end without the error decision crossing the threshold. In scenario 3, where the slope values are equal but the correct decision is delayed by 50 ms, the error decision will reach the threshold first and hence the subject once again will make the error prosaccade. It is clear from these scenarios that the race model is capable of only capturing two of the observed behaviours in the antisaccade task (i.e. behaviours (1) and (2)).

In a slightly modified version of the Race/LATER model, where the trial doesn't end when one of the decision signals exceeds the threshold value, but the trial continues when both decision signals cross the threshold, all three experimentally observed antisaccadic behaviours are observed in addition to a new fourth behaviour, where the error prosaccade follows the correct antisaccade. In this case it is obvious that an external inhibitory signal will be needed to stop the error prosaccade when the correct antisaccade is first expressed. The inhibitory signal can be avoided if the variability of error decision slope values is smaller than the variability of the correct decision slope values, ensuring that the decision signals never cross below the threshold. However, none of the above has ever been observed experimentally.

In our model, the lateral competition, which has been observed experimentally in the SC, between the two decision signals ensures that neither the external inhibitory signal nor the differences in slope variabilities of the two decision signals are needed to reproduce all three observed behaviours of the antisaccade task, if a 50 ms time delay between the two inputs (verified experimentally), a Gaussian distribution in input intensity (shown experimentally) and unequal maximal intensities of the two inputs (Ip $>$ Ir) are assumed. In scenario 1, the error signal will exceed first the threshold followed subsequently by (1) the correct signal or (2) no signal depending on the slope value of the correct decision signal. For instance, if the slope value of the correct signal is too small (less than 1), then the correct signal will most likely not have sufficient time to cross the threshold (remember SRTs $>$600 ms were thrown away (see Experimental Data section)). From this scenario, behaviours (2) and (3) are observed. In scenario 2, and since the correct signal is always greater in strength than

the error signal, only the correct antisaccade behaviour will be observed, since through lateral inhibition more inhibition from the correct antisaccade signal to the error prosaccade signal will prevent the latter from reaching the threshold. In scenario 3, the error prosaccade will be expressed first followed by the correct antisaccade. So, our model with dynamic competition and *no external top-down inhibitory signal* demonstrates all three observed behaviour in the antisaccade task and ensures that at no time we will observe the correct antisaccade been expressed after the error prosaccade.

4.4. Model limitations and failures

A major limitation of our model is that it offers no insight into the biophysical mechanisms that produce variable slopes in the integration of both decision signals by the buildup neurons of the SC and the formation of the categorical choice. The biophysical and circuit properties underlying operations such as integration are an active topic of investigation at the theoretical and experimental level (Cutsuridis, Kahramanoglou, Smyrnis, Evdokimidis, & Perantonis, 2007; Durstewitz, 2003; Wang, 2002). More recently, Cutsuridis et al. (2007) advanced a biophysical model which modelled the biophysically plausible mechanisms that produced climbing activity with adjustable slope. In that study, Cutsuridis et al. (2007) extended the present SC model by adding two cortical modules that generated the planned and reactive decision signals. The decision signals derived from the population activities of networks of pyramidal neurons and inhibitory interneurons. Hodgkin–Huxley mathematical formulations were used to model the population activities and explore the biophysical mechanisms in question. The model predicted that variability in the maximal conductances of specific ionic and synaptic currents (I_{NaP}, I_{NMDA} and I_{AMPA}) can reproduce the full range of slope values (see Table 2 herein) of the planned and reactive inputs of the SC model, while keeping the preset criterion level fixed. By reproducing the full range of the slope values, the model was implicitly able to generate the correct antisaccade and the error prosaccade reaction time (RT) distributions as well as the error prosaccade probabilities in the large group of 2006 men (Evdokimidis et al., 2002; Smyrnis et al., 2002) investigated in here.

4.5. Model extensions and alternatives

The analyses presented here show that the integration of sensory evidence to a threshold accounts for a wide variety of behavioural and physiological observations related to the antisaccade task. Several extensions to the basic idea deserve consideration. Variability in the parameters of integration, such as starting time and the baseline neuronal activity, may be helpful in improving the generality of the model, especially when incorporating prior biases into the decision (Carpenter & Williams, 1995). Similarly, the afferent delay between reactive and planned decision signals may be variable and is likely to change as a function of time. A dynamic afferent delay between inputs embodies the idea that commitment to one or another behavioural option may need to occur with some degree of urgency. These factors will need to be implemented into a more complete computational model.

Finally, work is underway in our laboratory to extend the present and the Cutsuridis et al. (2007) works and examine the effects of neurotransmitters such as dopamine (DA) on the *predicted* synaptic (I_{AMPA} and I_{NMDA}) and ionic (I_{NaP}) conductances of pyramidal neurons in the two cortical networks in order to study the performances of patients suffering from schizophrenia in the antisaccade task (Kahramanoglou, Cutsuridis, Smyrnis, Evdokimidis, & Perantonis, 2005, 2006).

Acknowledgements

The experimental data used come from a large ongoing cohort study supported by grant “EKBAN 97” to Professor C.N. Stefanis from the General Secretariat of Research and Technology of the Greek Ministry of Development.

References

Amari, S. (1997). Dynamics of pattern formation in lateral-inhibition type neural fields. *Biological Cybernetics*, *27*, 77–87.

Arai, K., Keller, E. L., & Edelman, J. A. (1994). Two-dimensional neural network model of the primate saccade system. *Neural Networks*, *7*, 1115–1135.

Asrress, K. N., & Carpenter, R. H. S. (2001). Saccadic countermanding: A comparison of central and peripheral stop signals. *Vision Research*, *41*, 2645–2651.

Basso, M. A., & Wurtz, R. H. (1998). Modulation of neural activity in superior colliculus by changes in target probability. *Journal of Neuroscience*, *18*, 7519–7534.

Becker, W. (1989). Metrics. In R. Wurtz, & M. Goldberg (Eds.), *Neurobiology of saccadic eye movements* (pp. 12–67). NY: Elsevier.

Becker, W. (1992). Saccades. In R. H. S. Carpenter (Ed.), *Vision and visual Dysfunction*: *vol. 8. Eye Movements* (pp. 95–137). London: MacMillan.

Behan, M., & Kime, N. M. (1996). Intrinsic circuitry in the deep layers of the cat superior colliculus. *Visual Neuroscience*, *13*, 1031–1042.

Britten, K. (2003). The middle temporal area: Motion processing and the link to perception. In W. J. Chalupa (Ed.), *The visual neurosciences*. Boston, MA: MIT Press.

Carpenter, R. H. (2000). The neural control of looking. *Current Biology*, *10*(8), R291–R293.

Carpenter, R. H. S., & Williams, M. L. L. (1995). Neural computation of log likelihood in the control of saccadic eye movements. *Nature*, *377*, 59–62.

Cutsuridis, V., Evdokimidis, I., Kahramanoglou, I., Perantonis, S., & Smyrnis, N. (2003). Neural network modeling of eye movement behavior in the antisaccade task: Validation by comparison with data from 2006 normal individuals. In *Society for Neuroscience Conference*.

Cutsuridis, V., Kahramanoglou, I., Smyrnis, N., Evdokimidis, I., & Perantonis, S. (2007). A neural variable integrator model of decision making in an antisaccade task. *Neurocomputing*, *70*, 1390–1402.

Dorris, M. C., Pare, M., & Munoz, D. (1997). Neural activity in monkey superior colliculus related to the initiation of saccadic eye movements. *Journal of Neuroscience*, *17*, 8566–8579.

Dormand, J. R., & Prince, P. J. (1980). A family of embedded Runge-Kutta formulae. *Journal of Computational and Applied Mathematics*, *6*, 19–26.

Durstewitz, D. (2003). Self-organizing neural integrator predicts interval times through climbing activity. *Journal of Neuroscience*, *23*(12), 5342–5353.

Durstewitz, D. (2004). Neural Representation of Interval Time. *Neuroreport*, *15*(9), 745–749.

Evdokimidis, I., Smyrnis, N., Constantinidis, T. S., Stefanis, N. C., Avramopoulos, D., Paximadis, C., et al. (2002). The antisaccade task in a sample of 2006 young men I. Normal population characteristics. *Experimental Brain Research*, *147*, 45–52.

Everling, S., Dorris, M. C., Klein, R. M., & Munoz, D. P. (1999). Role of primate superior colliculus in preparation and execution of anti-saccades and pro-saccades. *Journal of Neuroscience*, *19*(7), 2740–2754.

Everling, S., Dorris, M. C., & Munoz, D. P. (1998). Reflex suppression in the antisaccade task is dependent on prestimulus neural processes. *Journal of Neurophysiology*, *80*, 1584–1589.

Everling, S., & Fischer, B. (1998). The antisaccade: A review of basic research and clinical studies. *Neuropsychologia*, *36*, 885–899.

Fischer, B., & Weber, H. (1992). Characteristics of "anti" saccades in man. *Experimental Brain Research*, *89*, 415–424.

Funahashi, S., Chafee, M. V., & Goldman-Rakic, P. S. (1993). Prefrontal neuronal activity in rhesus monkeys performing a delayed antisaccade task. *Nature*, *365*, 753–756.

Godijin, R., & Theeuwes, J. (2002). Programming of endogenous and exogenous saccades: evidence for a competitive integration model. *Journal of Experimental Psychology*, *28*(5), 1039–1054.

Grammont, F., & Riehle, A. (1999). Precise spike synchronization in monkey motor cortex involved in preparation for movement. *Experimental Brain Research*, *128*, 118–122.

Grossberg, S. (1973). Contour enhancement, short term memory, and constancies in reverberating neural networks. *Studies in Applied Mathematics*, *52*, 213–257.

Grossberg, S., Roberts, K., Aguilar, M., & Bullock, D. (1997). A neural model of multimodal adaptive saccadic eye movement control by superior colliculus. *Journal of Neuroscience*, *17*, 9706–9725.

Hallett, P. R. (1978). Primary and secondary saccades to goals defined by instructions. *Vision Research*, *18*, 1279–1296.

Hanes, D. P., & Schall, J. D. (1996). Neural control of voluntary movement initiation. *Science*, *274*, 427–430.

Hikosaka, O., Takikawa, Y., & Kawagoe, R. (2000). Role of the basal ganglia in the control of purposive saccadic eye movements. *Physical Review*, *80*(3), 953–978.

Hikosaka, O., & Wurtz, R. H. (1983). Visual and oculomotor functions of monkey substantia nigra pars reticulata. II. Visual responses related to fixation of gaze. *Journal of Neurophysiology*, *49*, 1254–1267.

Hunt, A. R., Bettina, O., von Muhlenen, A., & Kingstone, A. (2004). Integration of competing saccade programs. *Cognitive Brain Research*, *19*, 206–208.

Kahramanoglou, I., Cutsuridis, V., Smyrnis, N., Evdokimidis, I., & Perantonis, S. (2005) Dopamine modification of climbing activity in a neural accumulator model of the antisaccade task. In: *1st Annual conference of computational cognitive neuroscience*.

Kahramanoglou, I., Cutsuridis, V., Smyrnis, N., Evdokimidis, I., & Perantonis, S. (2006) Dopamine effects on climbing activity of a cortico-tectal model: simulating the performance of patients with DSM-IV schizophrenia in the antisaccade task. In: *2nd Annual conference of computational cognitive neuroscience*.

Kim, J. N., & Shadlen, M. N. (1999). Neural correlates of a decision in the dorsolateral prefrontal cortex of the macaque. *Nature Neuroscience*, *2*(2), 176–185.

Kopecz, K. (1995). Saccadic reaction time in gap/overlap paradigm: a model based on integration of intentional and visual information on neural, dynamic fields. *Vision Research*, *35*, 2911–2925.

Kopecz, K., & Schoner, G. (1995). Saccadic motor planning by integrating visual information and expectation on neural dynamic fields. *Biological Cybernetics*, *73*, 49–60.

Leach, J. C. D., & Carpenter, R. H. S. (2001). Saccadic choice with asynchronous targets: Evidence for independent randomization. *Vision Research*, *41*, 3437–3445.

Luce, R. D. (1986). *Response times*. New York: Oxford University Press.

Matell, M. S., Mech, W. H., & Nicolelis, M. A. L. (2003). Interval timing and the encoding of signal duration by ensembles of cortical and striatal neurons. *Behavioral Neuroscience*, *117*, 760–773.

Mazurek, M. E., Roitman, J. D., Ditterich, J., & Shadlen, M. N. (2003). A role of neural integrators in perceptual decision making. *Cerebral Cortex*, *13*, 1257–1269.

Mazurek, M. E., & Shadlen, M. N. (2002). Limits to the temporal fidelity of cortical spike rate signals. *Nature Neuroscience*, *5*, 463–471.

McClelland, J. L. (1979). On time relations of mental processes: An examination of systems of processes in cascade. *Psychological Review*, *86*, 287–330.

McEchron, M. D., Tsend, W., & Disterhoft, J. F. (2003). Single neurons in CA1 hippocampus encode trace interval duration during trace heart rate (fear) conditioning in rabbit. *Journal of Neuroscience*, *23*, 1535–1547.

Meredith, M. A., & Ramoa, A. S. (1998). Intrinsic circuitry of the superior colliculus: Pharmacological identification of horizontally oriented inhibitory interneurons. *Journal of Neurophysiology*, *79*, 1597–1602.

Moschovakis, A., & Karabelas, A. (1985). Observations on the somatodedritic morphology and axonal trajectory of intracellularly HRP-labeled efferent neurons located in the deeper layers of the superior colliculus of the cat. *Journal of Comparative Neurology*, *239*, 276–308.

Moschovakis, A., Karabelas, A., & Highstein, S. (1988). Structure-function relationships in the primate superior colliculus. I. Morphological classification of efferent neurons. *Journal of Neurophysiology*, *60*, 232–262.

Munoz, D. P., & Everling, S. (2004). Look away: The antisaccade task and the voluntary control of eye movement. *Nature Reviews Neuroscience*, *5*, 218–228.

Munoz, D. P., & Fecteau, J. (2002). Vying for dominance: Dynamic interactions control visual fixation and saccadic initiation in the superior colliculus. *Progress in Brain Research*, *140*, 3–19.

Munoz, D. P., & Istvan, P. J. (1998). Lateral inhibitory interactions in the intermediate layers of the monkey superior colliculus. *Journal of Neurophysiology*, *79*, 1192–1209.

Munoz, D., & Wurtz, R. (1993). Fixation cells in monkey superior colliculus. I. Characteristics of cell discharge. *Journal of Neurophysiology*, *70*, 559–575.

Munoz, D., & Wurtz, R. (1995a). Saccade related activity in monkey superior colliculus. I. Characteristics of burst and buildup cells. *Journal of Neurophysiology*, *73*, 2313–2333.

Munoz, D., & Wurtz, R. (1995b). Saccade related activity in monkey superior colliculus. II. Spread of activity during saccades. *Journal of Neurophysiology*, *73*, 2334–2348.

Olivier, E., Dorris, M. C., & Munoz, D. P. (1999). Lateral interactions in the superior colliculus, not an extended fixation zone, can account for the remote distractor effect. *Behavioral and Brain Sciences*, *22*, 694–695.

Pare, M., & Munoz, D. P. (1996). Saccadic reaction time in the monkey: Advanced preparation of oculomotor programs is primarily responsible for express saccade occurrence. *Journal of Neurophysiology*, *76*(6), 3666–3681.

Parker, A. J., & Newsome, W. T. (1998). Sense and the single neuron: Probing the physiology of perception. *Annual Review of Neuroscience*, *21*, 227–277.

Ratcliff, R. (1979). Group reaction time distributions and an analysis of distribution statistics. *Psychological Bulletin*, *86*(3), 446–461.

Ratcliff, R., van Zandt, T., & McKoon, G. (1999). Connectionist and diffusion models of reaction time. *Psychological Review*, *106*, 261–300.

Reddi, B. A. J., Asrress, K. N., & Carpenter, R. H. S. (2003). Accuracy, information, and response time in a saccadic decision task. *Journal of Neurophysiology*, *90*, 3538–3546.

Reddi, B. A. J., & Carpenter, R. H. S. (2000). The influence of urgency on decision time. *Nature Neuroscience*, *3*, 827–831.

Roux, S., Coulmance, M., & Riehle, A. (2003). Context-related representation of timing processes in monkey motor cortex. *European Journal of Neuroscience*, *18*, 1011–1016.

Schall, J. D., & Hanes, D. P. (1998). Neural mechanisms of selection and control of visually guided eye movements. *Neural Networks*, *11*, 1241–1251.

Schultz, W., Dayan, P., & Montague, P. R. (1997). A neural substrate of prediction and reward. *Science*, *275*, 1593–1599.

Shook, B. L., Schlag-Rey, M., & Schlag, J. (1990). Primate supplementary eye field: I. Comparative aspects of mesencephalic and pontine connections. *Journal of Comparative Neurology*, *310*, 618–642.

Smyrnis, N., Evdokimidis, I., Stefanis, N. C., Constantinidis, T. S., Avramopoulos, D., et al. (2002). The antisaccade task in a sample of 2006 young males II. Effects of task parameters. *Experimental Brain Research*, *147*, 53–63.

Sparks, D. L. (1978). Functional properties of neurons in the monkey superior colliculus: Coupling of neuronal activity and saccade onset. *Brain Research*, *156*, 1–16.

Sparks, D. L. (2002). The brainstem control of saccadic eye movements. *Nature Reviews Neuroscience*, *3*(12), 952–964.

Taylor, J. G. (1999). Neural bubble dynamics in two dimensions: I. Foundations. *Biological Cybernetics*, *80*, 393–409.

Trappenberg, T. P., Dorris, M. C., Munoz, D. P., & Klein, R. M. (2001). A model of saccade initiation based on the competitive integration of exogenous and endogenous signals in the superior colliculus. *Journal of Cognitive Neuroscience*, *13*(2), 256–271.

Usher, M., & McClelland, J. L. (2001). The time course of perceptual choice: The leaky accumulator model. *Psychological Review*, *108*, 550–592.

Waitzman, D., Ma, T., Oprican, L., & Wurtz, R. (1991). Superior colliculus neurons mediate the dynamic characteristics of saccades. *Journal of Neurophysiology*, *66*, 1716–1737.

Wang, X. J. (2002). Probabilistic decision making by slow reverberation in cortical circuits. *Neuron*, *36*, 955–968.